Astron. Astrophys. 279, 447–456 (1993)

ASTRONOMY AND ASTROPHYSICS

The application of Monte Carlo methods to the synthesis of early-time supernovae spectra

P.A. Mazzali[1,2] **and L.B. Lucy**[3,⋆]

[1] European Southern Observatory, Karl-Schwarzchildstr. 2, D-85748 Garching bei München, Germany
[2] Osservatorio Astronomico, Via G.B. Tiepolo, 11, I-34131 Trieste, Italy
[3] ST-ECF, Karl-Schwarzschildstr. 2, D-85748 Garching bei München, Germany

Received August 29, 1992; accepted April 15, 1993

Abstract. The application of a Monte Carlo technique for treating multiline transfer in a supernova's expanding envelope and thereby computing synthetic early-time spectra is described.

The main physical assumptions are discussed, especially where they differ from the previous application to stellar winds. These include the calculation of the density and temperature stratification in the envelope, a more realistic treatment of ionization, and the treatment of radiative transfer on the assumption of a purely scattering atmosphere (Schuster–Schwarzschild model).

A detailed outline of the code, which has already been applied successfully to both SNe II and Ia, is also given, and the main advantages of using Monte Carlo methods for the synthesis of SN spectra are emphasized. These lie in the simplicity of the treatment of the multiline transfer, which is useful since line overlapping due to the large velocities reached by the expanding matter is common in a SN envelope; the implicit incorporation of line-blocking of the radiation field, which allows photoionization rates to be calculated straightforwardly; and the possibility of including relativistic effects easily. The isotropy of the expansion in SN envelopes also allows for simplicity and efficiency of the optical depth integrations.

The degree of self-consistency of our code is such that only basic parameters are required as input, so that the synthetic spectra yield valuable information on essential SN parameters such as the bolometric luminosity, the photospheric velocity and the effective wavelength of line formation.

Key words: radiation transfer – methods: numerical – supernovae: general

Send offprint requests to: P.A. Mazzali
⋆ Affiliated with Astrophysics Division, Space Science Dept., European Space Agency

1. Introduction

The application of Monte Carlo methods to the computation of synthetic spectra of expanding astrophysical gaseous envelopes was described by Abbott & Lucy (1985, hereafter AL). Compared to the formal solution approach (Castor 1970; Lucy 1971), the Monte Carlo approach allows a straightforward treatment of the otherwise numerically complex problem of the multiline transfer of radiation, which arises due to the varying velocity field in an expanding stellar envelope [e.g. Surdej (1980), Olson (1982) for the doublet problem; Puls (1987) for the general multiline problem; Mazzali (1990) for rotationally-induced multiline transfer].

AL tested the method for the case of the wind of the standard Of star ζ Puppis and showed that the empirically-determined mass loss rate and the observed far-UV spectrum could be successfully reproduced. The application of the method to the dense winds of WR stars is discussed in another paper (Lucy & Abbott 1993). The adaptation of the AL Monte Carlo code to treat the expanding envelopes of supernovae was prompted by SN 1987A (Lucy 1987, 1988). Later, in the context of the ESO Key Programme on supernovae (Cappellaro et al. 1991), further work has been done to improve the code's treatment of ionization and excitation, including the solution of a NLTE matrix for chosen elements (Mazzali et al. 1992), and to extend it to treat SNe Ia (Mazzali et al. 1993). Presently, the ESO Monte Carlo code is an efficient diagnostic tool for rapidly carrying out an initial coarse analysis of supernova spectra.

Theoretical spectral modelling is one of the most important approaches to the understanding of supernovae, since it allows one to investigate many of the properties of the SN envelope (luminosity, abundances, stratification, temperature, velocities, time evolution), as discussed for example by Mazzali et al. (1993).

The envelope of a supernova in the first few weeks after explosion is dense enough that the continuum optical

depth reaches unity within the envelope itself, giving rise to an effective photosphere that emits continuum radiation. This radiation is the result of the reprocessing within the inner part of the SN ejecta of the γ-rays emitted by the decay of the radioactive ^{56}Ni formed in the core of the SN progenitor during its collapse, when the stellar core is burned into nuclear statistical equilibrium. The γ-rays are degraded into UV, optical and IR photons by their interaction with the ejecta, and this makes the supernova event visible to the eye. The photospheric continuum radiation must then traverse the fraction of the envelope left above the photosphere, and thus interacts with the expanding gas in the envelope, just as the continuum radiation of a hot star does with the wind ejected by the star itself. The nature of the early-time (photospheric epoch) spectrum of a supernova is then analogous to that of a hot star's circumstellar spectrum, with the spectral lines taking the typical shape of P-Cygni profiles.

The multiline transfer typical of hot star winds becomes an even more extreme process in a SN envelope, where the velocities reached (up to $\sim 30\,000\ \mathrm{km\,s^{-1}}$) are much larger, so that a single continuum photon can interact with many more spectral lines by virtue of the progressive redshift of the photon in the comoving frame as the photon scatters in the differentially expanding envelope. The line overlap (Doppler overlapping) thus introduced establishes a radiative connection between different parts of the envelope, and makes the radiation transfer problem difficult for computational techniques based on the equation of radiative transfer. The line overlap is so large that in the UV the lines constitute a source of effective continuum opacity, an effect known as line-blocking. Thus, in the blue and UV the observed "emission peaks" are but the result of selected wavelength regions with relatively small line opacity where photons scattered by a large number of bluer spectral lines escape.

A Monte Carlo approach is therefore ideally suited in this case, while formal integral type solutions must explicitly take into account a very large number of lines simultaneously. In fact, our Monte Carlo code has proved successful in reproducing the spectra of both SNe II and Ia and yields very useful information on the global envelope characteristics. In this paper, we describe the major advantages of our code and its main features with respect to the solution of the physical problems inherent to the computing of synthetic supernova spectra (Sect. 2), and give a detailed description of the structure of the code (Sect. 3).

2. Model supernova envelope

In this section, we state and discuss the main assumptions necessary to make the Monte Carlo wind code of AL capable of handling a SN envelope, and the main changes to the adopted physics relative to AL.

2.1. Density stratification

The main difference between a stellar wind and a SN envelope lies in the density structure. A stellar wind has an asymptotic density dependence $\rho \propto r^{-2}$, from the continuity equation for a stationary flow, with a lower boundary density $\rho_{\rm ph}$ constant in time and determined to a very good approximation by that of a model atmosphere in radiative and mechanical equilibrium, since for weak winds (i.e. all except W–R winds) the photosphere barely knows about the wind. The density dependence of a supernova envelope, on the other hand, is determined by the explosion model, which changes for the different supernova types, and $\rho_{\rm ph}$ is not constant in time. In general, ρ drops much more steeply with radius in SNe than in stellar winds (in SNe Ia, typically, $\rho \propto r^{-7}$). The actual density values depend also on the ejecta's mass and on the position of the photosphere, which changes with time with respect to both radius and overlying mass. Since a SN outflow is not a steady state phenomenon, the photosphere recedes further and further into the envelope as expansion makes the density drop. In practice, the photosphere occurs at a roughly constant density.

We assume that the density has the profile given by a typical explosion model [e.g. W7 of Nomoto et al. (1984) for SNe Ia, or Arnett's (1988) model for SNe II]. This template density profile, calculated for a certain epoch, is expressed as $\rho(v)$ and is rescaled to the desired date assuming that the envelope is in a state of free, homologous expansion, i.e. that a parcel of matter in the ejecta moves at a constant velocity v and that v is a function of r such that $v=r/t$, where t is the time since the explosion. The position of the photospheric radius depends on the rescaled density and determines the structure of the "atmosphere" which continuum photons must travel through.

2.2. Temperature stratification

Once the envelope properties $[\rho(r), v(r)]$ have been determined, the behaviour of the temperature must be known before occupation number calculations can be performed. In the stellar wind case (AL), the simple assumption was made of isothermal flow with $T=0.9T_*$, where T_* is the photospheric effective temperature. In the case of a SN envelope, redshifts and backscattering cause the quality of the radiation to change with radius, with the hardness of the radiation decreasing as radius increases. It is important to take this variation into account, at least crudely. Thus, a simplified radiative equilibrium calculation is adopted.

The procedure used to compute the radiation temperature $T_{\rm R}$ is the following: the mean energy of a photon in a black body radiation field is given by

$$\bar{x}=\frac{h\bar{\nu}}{kT}, \tag{1}$$

with $\bar{x}=3.832$. Accordingly, in the Monte Carlo calcu-

lation we compute the frequency moment

$$\bar{\nu}=\frac{\int_0^\infty \nu J_\nu \, d\nu}{\int_0^\infty J_\nu \, d\nu}, \tag{2}$$

and assign an equivalent radiation temperature via Eq. (1), with $\bar{x}$ as above. (Note that had we chosen to work with the mean energy per photon, then we would have $\bar{\nu}=2.701$ and $\bar{\nu}=\int J_\nu \, d\nu / \int \nu^{-1} J_\nu \, d\nu$).

The calculation of the temperature structure is performed via the iteration between the occupation numbers and the radiation field obtained with the most recent value of T_R, until convergence is attained. The electron temperature is defined to be

$$T_e(r)=0.9T_R(r), \tag{3}$$

to simulate very approximately the radiative control of the electron temperature.

To start this iteration procedure, we take an initial temperature structure such that $T_R(r)=T_*$ throughout the envelope. T_* is obtained from the photospheric radius and velocity through the relation $L=4\pi R_*^2 \sigma T_*^4$.

The effect of viewing a finite photosphere and of the progressive degradation of the radiation upon its interaction with the envelope matter is such that $J(r)$ falls below $B(T_R(r))$. This allows us to compute an equivalent dilution factor W through:

$$J=WB(T_*)=W\frac{\sigma}{\pi}T_R^4. \tag{4}$$

In a code deliberately kept simple in order to carry out rapid coarse analyses of newly discovered SNe, one might expect that the temperature stratification would be derived from the condition $B=J$, i.e. by the application of gray atmosphere theory. However, this gives $T_e \sim (R_*/r)^{1/2}$ as $r \to \infty$, so that in the model's outer envelope the electron temperature would drop far below the radiation temperature. Accordingly, our procedure of setting $T_e=0.9T_R$, which crudely models the dominance of quality over quantity in the radiative control of the electron temperature, is preferred over the various available approximate treatments of extended gray atmospheres.

2.3. *Radiative transfer*

The next important assumption in our model is that we are dealing with a purely scattering envelope. Thus, we neglect continuum absorption, and assume, as in AL, that only line transitions and electron scatterings occur. This assumption implies that we adopt the Schuster–Schwarzschild approximation, i.e. that no continuum formation occurs above a sharply defined photosphere. In support of this assumption is the fact that SN envelopes typically have a steep outer density profile.

Spectral lines are also treated as scattering lines, with spontaneous decay to the original level following immediately any photon absorption. Thus, in both line and electron scattering events the number of identical photons in the sampled energy packet is conserved, and so is their comoving frequency ν', so that the packet's energy in the comoving frame is conserved. Accordingly, a packet's incident and emergent energies in the star's frame are related by

$$\varepsilon_{in}\left(1-\mu_{in}\frac{v}{c}\right)=\varepsilon_{out}\left(1-\mu_{out}\frac{v}{c}\right), \tag{5}$$

where μ_{in} and μ_{out} are the direction cosines in that frame and v is the envelope's velocity at the event's radius. The direction of the outgoing packet is chosen randomly as part of the Monte Carlo experiment, as described in Sects. 3.4 and 3.5.

The attenuation of a beam of radiation in the envelope along a distance s is given by

$$I_\nu(s)=I_\nu(0)\exp\left[-(\tau_e+\tau_L)\right], \tag{6}$$

where τ_e is the integrated optical depth due to electron scattering, which is simply:

$$\tau_e=\int_0^s \sigma_T n_e \, ds, \tag{7}$$

where σ_T is the Thomson electron scattering cross section and n_e is the electron density, which is calculated for the average ionization conditions in each of the shells in which the envelope is divided in our code, while τ_L is the integrated line optical depth. This is augmented only when the photon is brought into resonance with a spectral line due to the change of its comoving frequency ν' as it propagates through the envelope (i.e. the redshift induced by the envelope's motion). Thus, each Monte Carlo packet with a certain rest frequency ν interacts with lines of progressively lower frequency, regardless of its direction of motion, since in the SN envelope v is an increasing function of r, as in stellar winds, albeit with a different dependence. As in stellar wind work, then, it is convenient to treat this interaction in the narrow line limit (Sobolev approximation), assuming that the line-photon interaction takes place only at the specific point of resonance. This is a particularly sound assumption in a SN envelope, where the velocities are so large that the resonance region is very small compared to the scale length over which the envelope's physical properties (temperature, density, ionization) change significantly.

One major simplification compared to the stellar wind case is that in the SN envelope $v \propto r$, so that $dv/dr \equiv v/r$. The expression for the optical depth due to a single line [AL, Eq. (9)] then reduces to:

$$\tau_l=\kappa\rho\lambda\frac{r}{v}, \tag{8}$$

with

$$\kappa\rho = \frac{\pi e^2}{m_e c} n_l f_{lu}, \tag{9}$$

where all symbols have their usual meaning.

Whether an energy packet suffers line or electron scattering depends on the combined optical depth of these processes. This will be discussed in detail in the section on the numerical code.

2.4. *Ionization and excitation*

The ionization and excitation state of the envelope gas (i.e. of the level occupation numbers) is required for the computation of the line optical depths. In principle, this would require the simultaneous solution of the coupled equations of statistical equilibrium and radiative transfer. This is relatively simple when minor species only are dealt with, and an example of the application of this method is given in Mazzali et al. (1992). However, including a large number of ions in such a scheme, and species which dominate in abundance, would require the calculation of a large number of photoionization rates and an iteration process between radiation field and occupation numbers. Thus we have chosen to retain a simplified approach, similar to the one used by AL, who adopted the nebular approximation. Nevertheless, we have improved the treatment of the physical processes determining the occupation numbers where the AL method was clearly inadequate. This concerns in particular the treatment of ionization.

The essential improvement to the treatment of ionization is the inclusion of continuum opacity. AL assumed the expanding envelope to be optically thin in all ionization continua, and that the ionization equilibrium was determined by the balance between photoionization from the ground state only and radiative recombination to all levels, so that their ionization equation [AL, Eq. (11)] was:

$$\frac{n_{j+1} n_e}{n_j} = \zeta W \left(\frac{T_e}{T_R}\right)^{1/2} \left(\frac{n_{j+1} n_e}{n_j}\right)^*_{T_R}, \tag{10}$$

where the starred terms mean LTE. This is similar to the standard nebular equation [Mihalas 1978, Eq. (5–46)], apart from the factor ζ, which represents the fraction of recombinations going directly to the ground state. The equation can be easily derived from the nebular case making the assumption of ground state ionization only. All the other symbols have their usual meaning (W is the dilution factor).

The first step of our improved treatment is to consider ionization from excited levels as well as from the ground state. The excited level's populations are computed as in AL using the diluted radiation field $J_\nu = WB_\nu$ determined as described in Sect. 2.2. The ionization equation becomes then

$$\frac{n_{j+1} n_e}{n_j} = W[\zeta + W(1-\zeta)] \left(\frac{T_e}{T_R}\right)^{1/2} \left(\frac{n_{j+1} n_e}{n_j}\right)^*_{T_R}, \tag{11}$$

where the added term $W^2(1-\zeta)$ represents photoionizations from excited levels. The extra factor W is introduced to describe approximately the excited level population (AL).

Next, we introduce the concept of an optically thick continuum at wavelengths shorter than that of the first major ionization edge. This is a sound approximation because the UV continuum, where most ionization edges occur, is known from observations to be optically thick. If we assume that the first major ionization edge encountered going towards shorter wavelengths has energy $\chi_0 = h\nu_0$, we can divide the spectrum into two regions, where the radiation field has different forms

$$J_\nu = WB_\nu(T_R) \quad \text{for } \nu < \nu_0 \tag{12}$$

and

$$J_\nu = b_1^{-1} B_\nu(T_e) \quad \text{for } \nu \geq \nu_0, \tag{13}$$

where b_1 is a weighted mean departure coefficient for the ground states of the ions that make the envelope opaque at high frequencies. Thus we assume that in the optically thin continuum the radiation field has the form of a diluted black body at the local radiation temperature, while in the optically thick continuum, where $J_\nu < B_\nu(T_e)$ and $T_R < T_e$, it is the locally emitted ($W = 1$) black body, whose shape is determined by T_e, with depleted photon density when $b_1 > 1$.

The ionization equation must then be rewritten to take into account that for $\nu \geq \nu_0$ the Saha equation, which holds in the optically thick region, must be recovered, while in the optically thin region $\nu < \nu_0$ the approximate Saha equation described above still holds. We assume that photoionizations from all excited levels always occur at frequencies where the continuum is optically thin. This approximation is of course not necessarily valid for all excited levels, especially those that lie near the ground state, but we nevertheless adopt it as a necessary simplification since these levels typically contain only a fraction of an ion's population. We thus introduce a correction factor δ in the ionization equation, and write:

$$\frac{n_{j+1} n_e}{n_j} = W[\delta\zeta + W(1-\zeta)] \left(\frac{T_e}{T_R}\right)^{1/2} \left(\frac{n_{j+1} n_e}{n_j}\right)^*_{T_R}. \tag{14}$$

The correction factor δ can take on two different values. If a species' ground state ionization threshold $\chi_T \geq \chi_0$, all ionising photons for that species' ground state fall in the optically thick continuum. Since the Saha equation must be recovered then, we have

$$\delta = \frac{T_e}{b_1 W T_R} \exp\left(\frac{\chi_T}{kT_R} - \frac{\chi_T}{kT_e}\right), \tag{15}$$

such that the ionization equation becomes

$$\frac{n_{j+1} n_e}{n_j} = \zeta \left(\frac{n_{j+1} n_e}{n_j}\right)^*_{T_e} + W^2(1-\zeta) \left(\frac{T_e}{T_R}\right)^{1/2} \left(\frac{n_{j+1} n_e}{n_j}\right)^*_{T_R}. \tag{16}$$

This recovers the Saha equation for the ground state ionization (first term), while photoionization from excited levels still follows the approximate Saha treatment.

If on the other hand, $\chi_T < \chi_0$, then an ionising photon can either have energy $h\nu \geq \chi_0 > \chi_T$ and lie in the optically thick continuum, or it can have energy $\chi_0 > h\nu \geq \chi_T$ and lie in the optically thin continuum. We then write the photoionization rate in two parts as follows:

$$R_{i\kappa} = 4\pi \int_{\nu_T}^{\nu_0} \alpha_\nu \frac{W B_\nu(T_R)}{h\nu} \, d\nu + 4\pi \int_{\nu_0}^{\infty} \alpha_\nu \frac{B_\nu(T_e)}{b_1 h\nu} \, d\nu, \quad (17)$$

where the subscript κ stands for processes involving the continuum, and α_ν is the photoionization cross section. If we now take the Wein limit $h\nu \gg kT_e$ for B_ν, and assume $\alpha_\nu = \alpha_T(\nu_T/\nu)^2$, where α_T is the photoionization cross section at threshold, we obtain

$$\begin{aligned} R_{i\kappa} &= \frac{8\pi}{c^2} \alpha_T \nu_T^2 \left[W \int_{\nu_T}^{\nu_0} \exp\left(-\frac{h\nu}{kT_R}\right) d\nu \right. \\ &\quad \left. + \frac{1}{b_1} \int_{\nu_0}^{\infty} \exp\left(-\frac{h\nu}{kT_e}\right) d\nu \right] \\ &= \frac{8\pi}{c^2} \alpha_T \nu_T^2 \left\{ W \frac{kT_R}{h} \left[\exp\left(-\frac{h\nu_T}{kT_R}\right) - \exp\left(-\frac{h\nu_0}{kT_R}\right) \right] \right. \\ &\quad \left. + \frac{kT_e}{b_1 h} \exp\left(-\frac{h\nu_0}{kT_e}\right) \right\}. \quad (18) \end{aligned}$$

If we compare this with the result of the AL nebular approximation,

$$R_{i\kappa} = \frac{8\pi}{c^2} \alpha_T \nu_T^2 W \frac{kT_R}{h} \exp\left(-\frac{h\nu_T}{kT_R}\right), \quad (19)$$

we see that the correction factor for ground state ionization is

$$\delta = 1 - \exp\left(\frac{h\nu_T}{kT_R} - \frac{h\nu_0}{kT_R}\right) + \frac{T_e}{b_1 W T_R} \exp\left(\frac{h\nu_T}{kT_R} - \frac{h\nu_0}{kT_e}\right). \quad (20)$$

The model of the radiation field assumes the envelope to be optically thick at high frequencies. The radiation field is then locally created, but is nevertheless physically diluted relative to the Planck function, due to the overpopulation of the ground states (Castor 1979). In our calculations, we set the departure coefficient $b_1 = W^{-1}$. This is consistent with the assumption made in Eq. (13), and is expected to be a reasonable approximation if $T_e \sim T_R$ throughout the envelope. Despite the inclusion of these additional effects, our ionization formula remains at best a crude first approximation.

The approximation regarding the nature of the radiation field requires a careful selection of the χ_0 value. For SNe II, where hydrogen is the main constituent of the envelope, the choice $\lambda_0 = 912$ Å is an easy guess. For SNe Ia, where several edges are important, $\lambda_0 = 1050$ Å can be chosen as an educated guess, to include the CaII edge, the redmost of the important edges. These selections neglect the effect of line-blocking, which makes the UV continuum partially optically thick at wavelengths longer than those given above. This is clearly shown by the observed spectra, which are black in the far-UV and rise only slowly to a typical black body-type continuum at longer wavelengths. This effect could be mimicked by adopting, in the region between say 1000 and 2500 Å a radiation field resulting from some sort of interpolation between the two limiting continuum types but, since not many ions have ionization edges in this wavelength region, we have chosen to ignore this effect, but to take it into account explicitly if actual NLTE calculations are performed (Mazzali et al. 1992). The principal effect of line-blocking is in fact to reduce photoionization from excited levels, not from ground states, and this can only be taken into account if a full occupation number matrix is solved. Indeed, the application of our ionization calculation method of both SNe II (Mazzali et al. 1992) and SNe Ia (Mazzali et al. 1993) has shown that the method can describe satisfactorily the ionization structure for the dominant ions, while it may need improvement for the minor species. The calculation of the excitation state of the envelope gas is unchanged with respect to the treatment described by AL.

3. Numerical technique: the Monte Carlo code

In this section we describe the steps necessary to compute an early-time supernova spectrum with our Monte Carlo code. The main assumption of the code is that the Schuster–Schwarzschild approximation holds, i.e. that no energy deposition occurs in the envelope above a sharply defined photosphere. The main steps of our code are the definition of the photospheric parameters, the calculation of the envelope properties, the selection of the relevant spectral lines, and the computation of the radiative transfer and thus of the emergent spectrum.

3.1. Input data

Only the very basic parameters are required as input by the code. A template SN density profile and the time t from explosion are necessary to rescale the density structure as described in Sect. 2.1. The photospheric radius, R_{ph}, i.e. the envelope's lower boundary, and the photospheric luminosity, L_{ph}, are needed to compute the temperature structure. Finally, an abundance file must be used for the optical depth calculation. The abundances can be a function of radius.

R_{ph} and L_{ph} define a photospheric effective temperature T_*. The envelope is then divided into a number of concentric shells, within each of which the physcial properties are assumed to be constant and equal to those at the shell's mid-point. Only the velocity remains a continuous function of radius because of its role in determining the location of line scatterings.

3.2. Line selection

The first necessary step is to select from a large database those lines which will be important for the given envelope conditions. We use typically Abbott's (1982) line list, which contains about 10^5 lines important for hot star winds, supplemented by the lines from the list of Kurucz & Petreymann (1975) for species of lower ionization and for elements not included in Abbott's list (Lucy 1987). Errors in wavelength of *gf* values and missing lines have been corrected as we became aware of them. A first rough estimate of the temperature structure in the envelope is then obtained setting $T_R = 1.4 - 0.4(1 - R_{ph}/r)T_*$ and $T_e(r) = 0.9T_R(r)$. The dilution factor is calculated from its geometrical definition, $W = \frac{1}{2}[1 - (1 - (R_{ph}/r)^2)^{1/2}]$, and these values are used for the first ionization structure calculation. Then the optical depth of all lines in our database is calculated, and those lines which are stronger than an arbitrarily chosen value, typically 0.001, in at least one shell, are retained for the Monte Carlo calculation.

3.3. Determination of the temperature structure

After the line selection, a temperature structure must be defined so that the occupation numbers and the line optical depths can be calculated. This is done iteratively with a series of small Monte Carlo experiments, as described in Sect. 2.2. The first guess is to set T_R constant and equal to $T_\star$, while $T_e = 0.9T_R$. Successive Monte Carlo iterations with a small number of energy packets allow us to compute $T_R(r)$ using the approximate radiative equilibrium method discussed in Sect. 2.2. Details of the Monte Carlo method are given in the next section. A temperature structure converged to the 1% level is usually obtained within ~ 10 iterations, using ~ 2000 energy packets in each iteration. This is a reasonably quick computation on a standard unix-type machine. Lack of convergence usually indicates that the input parameters are not self-compatible (e.g. L_{ph} too high for a given R_{ph}). As usual T_e is set at $0.9T_R$.

The calculation of a converged temperature structure in the envelope using an approximate radiative equilibrium method leads also to the determination of the temperature of the photospheric black body necessary to produce the required luminosity. This value T_B is usually higher than T_*, since a considerable fraction of the photons emitted at the photosphere eventually re-enter the photosphere itself after a series of scattering events in the envelope. This effect, known as backwarming, leads to an increased temperature gradient at and above the photosphere.

Once the converged temperature structure has been obtained, all the data necessary for the computation of the radiative transfer and of the emergent spectrum – i.e. the main Monte Carlo experiment – have been gathered.

3.4. Radiative transfer

This is the main part of the model computation, and is performed in the Sobolev approximation. In the MC code, the scattering histories of a number of energy packets are followed. The packets are chosen to have all the same initial energy, so that the photospheric luminosity L_{ph} is divided evenly among them, regardless of their frequency. If there are N packets, then each packet has energy $\varepsilon = L_{ph}/N$, which means that each packet represents a number of photons n_ν, where $n_\nu h\nu = \varepsilon$. The number of packets in any frequency interval depends then on what fraction of the photospheric luminosity is emitted in that frequency range. The distribution of the packets with frequency is determined by sampling the Planck function $B_\nu(T_*)$ with a number of frequency bins, imposing the constraint that each bin contains an integer number of packets of energy ε. This technique, known as stratified sampling, damps Poisson fluctuations, and for supernovae gives a smooth continuum. Using energy packets rather than photons allows one to sample the radiation field more accurately at the wavelengths where the bulk of the energy emerges and to avoid following an unnecessarily large number of IR photons.

The N energy packets are thus created at the photosphere. The frequency of each packet is assigned randomly within the appropriate bin, by generating a random number z between 0 and 1 and setting $\nu = \nu_{min} + z(\nu_{max} - \nu_{min})$. The direction of emission is also assigned randomly as a direction cosine $\mu = \sqrt{z}$, which gives the correct distribution of direction cosines for emission with zero limb-darkening from a surface. In practice, since random number generator routines yield $0 \le z < 1$, we use $\mu = (1 - z)^{1/2}$.

The scattering history of each packet is then followed. In a purely scattering envelope the fate of a photon (or energy packet) emitted at the photospheric boundary can be one of only two options: either the photon is scattered back into the photosphere after one or many line or electron scattering events, or it escapes the envelope, most likely after suffering a number of scatterings. A schematic diagram of a photon's travel was shown in AL (their Fig. 5). Deciding whether a packet suffers a line or electron scattering, and what happens to it after such events, is the basic task performed by the Monte Carlo code.

When a packet is emitted at the photosphere with a frequency ν and a direction cosine μ in the rest frame, it finds itself in the first of the physically homogeneous shells into which the envelope has been divided. A convenient number of shells is typically 10–20. The name of the Monte Carlo game is then to decide whether the packet will be scattered by a line or an electron before it can cross that shell's outer boundary and enter the next shell, where the physical conditions are different. The direction of ejection is then used to calculate the distance the packet must travel to reach the outer edge of the first shell. In order to decide whether a scattering event will take place within the

first shell, a random "event" optical depth is selected with the formula $\tau_R = -\ln(z)$, where z is a random number between 0 and 1. Since random number generating routines return values $0 \leq z < 1$, the expression is replaced with $\tau_R = -\ln(1-z)$. Then the two possible event types are considered. Electron scattering occurs with a probability that is a linear function of distance if, as is the case within a single shell, the electron density is constant. Line scattering, on the other hand, can occur only at specific points along the photon's trajectory, where the envelope's motion brings the packet into resonance with a spectral line (Sobolev approximation). Given the expanding nature of the envelope's motion, a packet emitted at the photosphere with a certain rest wavelength can only interact with lines of longer wavelength. The positions of the resonance surfaces can be easily calculated.

The optical depth encountered by the photon during its flight is computed as follows: initially, the photon travels freely to its next line scattering, but during this flight it encounters an electron scattering optical depth τ_e. The length of the path s_e the photon can travel freely before τ_e becomes equal to the randomly selected event optical depth τ_R is calculated using the formula $\tau_R = \sigma_T n_e(i)$ s_e, where $n_e(i)$ is the electron density of the ith shell. The formula assumes the electron density to be constant, and is therefore valid only within a single shell. If s_e is less than the distance needed to exit the shell, the photon may suffer electron scattering in the shell. Next, s_e is compared to the distance to the next line encounter, s_ℓ. This is easily calculated in terms of the photon's comoving frequency at the resonance point, $\nu' = \nu[1 - \mu(v/c)]$, using the Doppler formula with $v \propto r$.

Now the distances to the edge of the shell, s_{sh}, to the next electron scattering, s_e, and to the next line scattering, s_ℓ, must be compared. The next event in the photon's history will be the one that occurs at the shortest distance. If s_{sh} is such value, the photon enters the next shell, and a brand new optical depth calculation must begin. If the event is an electron scattering, the packet is assigned a new random direction at the scattering point, and a new Monte Carlo game starts. Finally, if the next event is a line scattering, the line optical depth τ_ℓ must be calculated from the occupation numbers. If the sum of τ_ℓ plus the electron scattering optical depth τ_e encountered during the flight to the line scattering [i.e. $\tau_e = \sigma_T n_e(i) s_\ell$] exceeds the event optical depth τ_R, line scattering occurs, otherwise the packet travels to the next line encounter, and new τ_e's and τ_ℓ's are added until either the sum of all τ_e's and τ_ℓ's exceeds τ_R, in which case an event occurs, or the packet leaves the shell. This process is shown in Fig. 1. The random optical depth τ_R defines the event's position in a τ coordinate, τ_e's and τ_ℓ's are summed, and electron or line scattering occurs depending on which particular contribution makes τ_{tot} become equal to or greater than τ_R. In the course of this process, τ_e grows continuously, while τ_ℓ is only augmented at the specific resonance locations.

In practice, since a large number of scatterings within a single shell makes the code run slowly, and since the velocity range in a SN envelope is so large that fine spectral details cannot be observed, it may be convenient

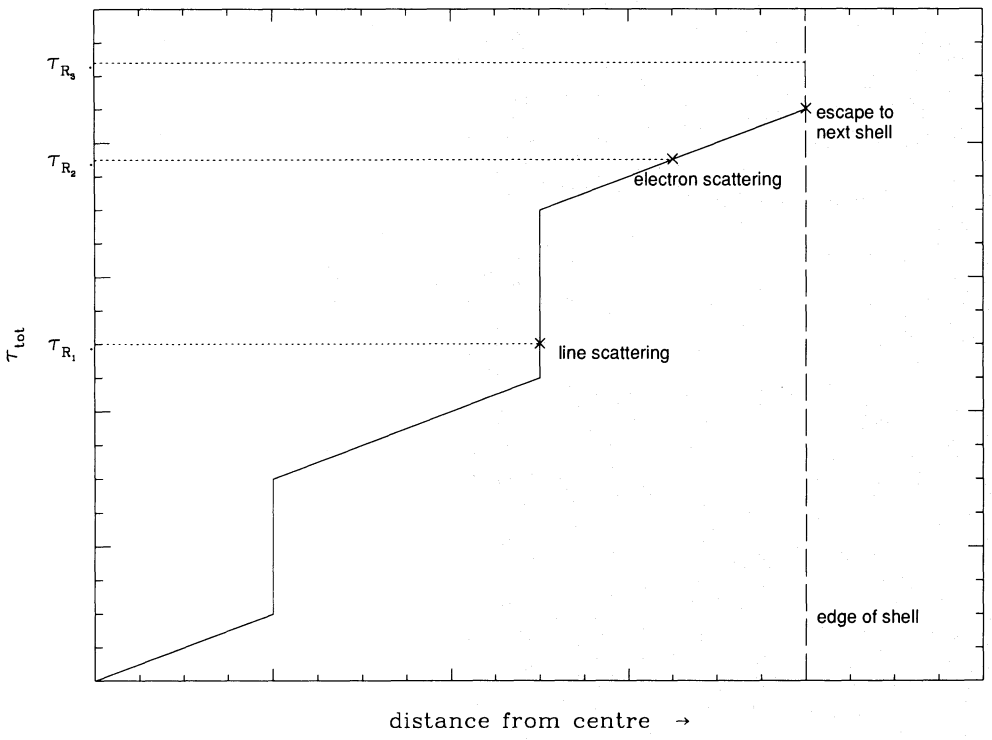

Fig. 1. The optical depth summation procedure. The electron scattering optical depth τ_e grows linearly with distance travelled by the energy packet, while the line optical depth τ_ℓ is only augmented at the resonance points (Sobolev approximation). Once a random event optical depth τ_R has been selected as the termination of the packet's next free flight, the occurrence of line or electron scattering depends on which of the two contributions makes the total optical depth τ_{tot} grow above τ_R. Two such examples are shown (cases τ_{R_1} and τ_{R_2}). If the selected τ_R is higher than the integrated optical depth in the shell (case τ_{R_3}) the photon escapes to the next shell

to sum the τ_ℓ's of several lines lying close in wavelength before the Monte Carlo game starts, and to consider thus only "line packets" in the radiative transfer calculation. However, this further improvement in efficiency has not been implemented.

The computation of τ_ℓ is made simple by the isotropy of the SN envelope, which eliminates the need to calculate directional derivatives of the velocity field since $v \propto r$. This same trick can be used in stellar wind calculations if the division into shells is fine enough that μ changes negligibly during a packet's free flight through a shell, and is in fact used in the calculations of Lucy & Abbott (1993).

3.5. Scattering events

Upon a scattering event, a new direction cosine must be calculated as a random number between -1 and $+1$ in the comoving frame, since scattering is isotropic, as required by Sobolev theory in the case when $dv/dr = v/r$, which holds in SN envelopes. This is done by setting $\mu' = 1 + 2z$. (Primed quantities are measured in the comoving frame, while unprimed ones are measured in the rest frame.) Scattering conserves comoving energy and frequency. The comoving frame frequency is related to the rest frame frequency by the relation:

$$\nu' = \nu\gamma\left(1 - \mu\frac{v}{c}\right), \tag{21}$$

with $\gamma = [1-(v^2/c^2)]^{-1/2}$, while the relation for the packet's energies in the two frames is

$$\varepsilon' = \varepsilon\frac{\nu'}{\nu}. \tag{22}$$

Since for scattering $\varepsilon'_{\rm in} = \varepsilon'_{\rm out}$, the rest frame energies are related by

$$\varepsilon_{\rm in}\left(1 - \mu_{\rm in}\frac{v}{c}\right) = \varepsilon_{\rm out}\left(1 - \mu_{\rm out}\frac{v}{c}\right), \tag{23}$$

where $\mu_{\rm in}$ and $\mu_{\rm out}$ are the incident and emergent direction cosines in the rest frame. The relation between direction cosines in the rest and comoving frames is

$$\mu = \frac{[\mu' + (v/c)]}{[1 + \mu'(v/c)]}. \tag{24}$$

The photon's frequency in the rest frame is then

$$\nu_{\rm out} = \nu_{\rm in}\frac{\varepsilon_{\rm out}}{\varepsilon_{\rm in}}. \tag{25}$$

The above transformations, which have been given for the fully relativistic case, can be easily simplified to be accurate to $\mathcal{O}(v/c)$, which is sufficient if the envelope velocities are not exceedingly large, by simply setting $\gamma = 1$, so that Eq. (21) becomes:

$$\nu' = \nu\left(1 - \mu\frac{v}{c}\right). \tag{26}$$

3.6. Calculation of integrated moments

The Monte Carlo experiment following a packet's propagation within a shell with uniform physical properties terminates when the photon eventually leaves the shell. This may happen either in an upward or in a downward direction (forward and backward scattering are allowed). If the packet crosses the photospheric boundary in a downward direction it is reabsorbed in the photosphere's thermal pool, and it is effectively lost. The loss of photons due to backscattering is an important effect in a SN envelope due to the large velocities, which force a photon to interact with a large number of lines. In the UV, lines are so crowded that they represent effectively a source of continuum opacity, giving rise to the effect known as line-blocking. Our Monte Carlo code deals with line-blocking implicitly, as discussed by Mazzali et al. (1992), and is therefore a particularly well suited method for treating such high velocity envelopes.

Whenever a packet crosses a shell's mid-point, its contribution to that shell's integrated moments of the radiation field can be computed. The specific intensity in the star's frame is given by

$$I_\nu\,\Delta\nu\,\Delta\omega = \frac{n\varepsilon}{\Delta t|\mu|} \tag{27}$$

for n energy packets with frequencies in the interval $\Delta\nu$ crossing unit area with solid angle $\Delta\omega$ and propagating in a direction inclined at an angle $\cos^{-1}\mu$ to the radius vector in unit time Δt. The corresponding estimator for the specific intensity in the comoving frame is obtained by applying the transformation properties of I_ν and $d\nu\,d\omega$: $I_\nu = (\nu/\nu')^3 I'_{\nu'}$ and $d\nu\,d\omega = (\nu'/\nu)\,d\nu'\,d\omega'$ (e.g. Mihalas 1978, Ch. 14-3). The result is

$$I'_{\nu'}\,\Delta\nu'\,\Delta\omega' = \frac{n\varepsilon}{\Delta t|\mu|}\left(\frac{\nu'}{\nu}\right)^2. \tag{28}$$

Estimators for moments in either frame are now readily derived. For example, summing Eq. (28) over all packets that cross the unit area $\Delta\omega$ and then averaging over the $4\pi r^2$ equivalent areas, we obtain

$$J' = \frac{1}{16\pi^2 r^2}\frac{1}{\Delta t}\sum\frac{\varepsilon}{|\mu|}\left(\frac{\nu'}{\nu}\right)^2 \tag{29}$$

as an estimator for the integrated mean intensity in the comoving frame. Formulae for higher moments in this frame are obtained by including the appropriate powers of the direction cosine μ'. Note also that including the factor $\kappa'_{\nu'}$ in the above summation yields an estimator for the quantity $\int_0^\infty \kappa'_{\nu'} J'_{\nu'}\,d\nu$, which can be used in a radiative equilibrium calculation. Also, the integration of $J'_{\nu'}$ in the appropriate frequency regime allows the radiation field contributing to the various photoionization rates to be explicitly calculated. Since line-blocking is implicitly included in our Monte Carlo code, these rates can be directly

used for the calculation of NLTE occupation numbers (Mazzali et al. 1992).

A quantity of importance in the rest frame is $L(r)$, the luminosity at r. From Eq. (27) its estimator is readily found to be

$$L=\frac{1}{\Delta t}\sum \varepsilon \frac{\mu}{|\mu|}. \tag{30}$$

We note that L is not constant with radius because of the redshift imposed by the velocity field, unlike the case of static atmospheres.

Finally, the calculation of the integrated mean intensity, J', and of the related quantity $\int_0^\infty \nu' J'_\nu \, d\nu$ is useful for the approximate radiative equilibrium calculation [Eq. (2)]. All the moments can be conveniently normalised in terms of the flux F_* or the luminosity $L_{\rm ph}$.

3.7. *The emergent spectrum*

All packets that are not reabsorbed at the photosphere must eventually escape, since the envelope is of a purely scattering type in our model. On average, escaping packets will be redshifted, in the rest frame, and more photons will escape in the wavelength regions where the line opacity throughout the envelope is smaller. In any case, the energy distribution of the escaping photons reflects the history of the photons' travel through the envelope. This constitutes the emergent spectrum, which is the final result of the calculation and which can be compared to the observations.

One further piece of information can be obtained from the code: the effective formation wavelength and the total optical depth of the lines included in the model. This information is necessary for the identification of the lines present in the spectrum, and can be obtained straightforwardly once the optical depth of the lines is known in all the shells in which the envelope has been subdivided.

If a line has optical depth τ_i in the ith shell, the fraction of the incoming radiation which is scattered upon encounter with a line is $1-\exp(-\tau_i)$. If v_i is the velocity at the shell's lower boundary, then the velocity width of the shell is $\Delta v_i = v_{i+1}-v_i$. A narrow spectral line with rest wavelength λ_0 can then interact in that shell with photons with wavelength from $\lambda_i=\lambda_0(1-v_i/c)$ to $\lambda_{i+1}=\lambda_0(1-v_{i+1}/c)$, i.e. in a wavelength interval $\Delta\lambda_i=\lambda_0\Delta v/c$. The amount of radiation absorbed by a line within the ith shell can therefore be approximated as

$$W_i=\Delta\lambda_i(1-e^{-\tau_i}). \tag{31}$$

This is expressed in wavelength units, and is a sort of line equivalent width. W_i is in fact larger for larger τ_i and for larger $\Delta\lambda$, i.e. if the velocity dispersion is large. In this case the line is effective in a large rest frame wavelength range, and can thus avoid saturation effects and block more of the incoming radiation. The total equivalent width of a line is then $\Sigma_i W_i$.

The line formation wavelength is an approximation for the wavelength at which an observer records the absorption core of the line. This will obviously be blueshifted with respect to the line's rest frame wavelength, since the feature is the absorbtion part of a P-Cygni profile. The blueshift will reflect roughly the velocity of the region where the line is strongest. If we assume that in each shell the average rest frame wavelength of a photon resonant with the transition considered is $\lambda_i=\lambda_0[1-(v_{i+1/2}/c)]$, where $v_{i+1/2}$ is the velocity of the shell's mid-point, then the line formation wavelength can be approximately found using the mean:

$$\lambda_{\rm obs}=\frac{\Sigma_i\lambda_i(1-e^{-\tau_i})\Delta\lambda_i}{\Sigma_i(1-e^{-\tau_i})\Delta\lambda_i}. \tag{32}$$

With this method a list of observed lines, their wavelengths and relative strengths is easily obtained.

The blueshift of the line formation wavelength is usually larger the stronger the line considered, and it may also reflect changes in ionization fractions within the envelope. This should warn against the use of the observed wavelength shifts of the absorption features as a measure of the photospheric velocity, for which such shifts give at most an upper limit. It would of course be safer to use weak lines, instead of the usual strong ones, but these are seldom unaffected by blends, and are very sensitive to ionization effects. Only the accurate matching of the observed and model wavelengths, resulting from the computation of a successful model, allows an estimate of the photospheric velocity to be made, as discussed by Mazzali et al. (1993).

Finally, the model spectrum's flux must be reduced by the distance attenuation factor, $(4\pi d^2)^{-1}$, and reddened with an appropriate law before it can be compared with observations.

4. Conclusions

We have discussed the problems related to the use of a Monte Carlo code for the synthesis of SN spectra, and have given a detailed description of our code, which has been successfully applied to both SNe II and Ia (Mazzali et al. 1992, 1993). The code needs as input only a few parameters, i.e. the photospheric velocity, radius and luminosity, the chemical composition of the envelope, a template density stratification and the time from outburst at which the spectrum must be computed, the distance and reddening to the object of interest. From these values, the code computes consistently a velocity, temperature and density stratification for the particular SN type, the ionization structure in the envelope, and finally the observed spectrum and a list of observed lines, their Sobolev optical depths and their formation wavelengths. All this information can be used fruitfully for spectral diagnostics which, given the degree of self-consistency of our code, can address not only line identification and abundance issues, but also give reliable insight on the photospheric velocity, the

ionization stratification and, perhaps most importantly, the bolometric luminosity of a supernova.

The main areas where the code may still be improved are essentially two: the treatment of ionization, where our scheme, although it is already farily realistic, still falls short of an exact NLTE treatment, which would ideally be required, and the line database, which is not complete in the present state. Still, the results obtained with the code are very satisfactory, and we plan to use the code extensively in the future to study supernovae of all types.

As stressed earlier, the code herein described is designed to provide a rapid, coarse spectral analysis of newly discovered supernovae that can be included already in discovery papers. Of course, if warranted by the astrophysical importance of the particular SN and the quality of the accumulated data, such a coarse analysis should be followed by a fine analysis with a NLTE code. However, in view of the growing evidence that the mixing out of ^{56}Ni is common, the NLTE code should not assume that γ-ray thermalization is complete below the photosphere: non-thermal excitation and ionization should be included as well as departures from thermal equilibrium due to energy deposition in the atmospheric layers.

Acknowledgements. This work was conducted as part of the ESO Key Programme on Supernovae.

References

Abbott D.C., 1982, ApJ 259, 282
Abbott D.C., Lucy L.B., 1985, ApJ 288, 679
Arnett W.D., 1988, ApJ 331, 377
Cappellaro E., Bouchet P., Della Valle M., et al., 1991, in: Danziger I.J., Kjär K. (eds.) SN 1987A and other Supernovae, ESO Conf. Proc. 37. ESO, Garching, p. 623
Castor J.I., 1970, MNRAS 149, 111
Castor J.I., 1979, in: Conti P.S., de Loore C.W.H. (eds.) IAU Symp. 83: Mass loss in Evolution of O-type Stars. Reidel, Dordrecht, p. 175
Kurucz R.L., Petreymann E., 1975, Smithsonian Ap. Obs. Special Report 362
Lucy L.B., 1971, ApJ 163, 95
Lucy L.B., 1987, in: Danziger I.J. (ed.) ESO Workshop on SN 1987A, p. 417
Lucy L.B., 1988, in: Kafatos M., Michalitsianos A. (eds.) Cambridge University Press, Cambridge, p. 323
Lucy L.B., Abbott D.C., 1993, ApJ 405, 738
Mazzali P.A., 1990, A&A 238, 191
Mazzali P.A., Lucy L.B., Butler K., 1992, A&A 258, 399
Mazzali P.A., Lucy L.B., Danziger I.J., et al., 1993, A&A 423, 269
Mihalas D., 1978, Stellar Atmospheres, 2nd ed. Freeman, New York
Nomoto K., Thielemann F.-K., Yokoi K., 1984, ApJ 286, 644
Olson G.L., 1982, ApJ 255, 267
Puls J., 1987, A&A 184, 227
Surdej J., 1980, ApSS 73, 101